Journal of Materials Science: Materials in Electronics (2019) 30:2489–2500
https://doi.org/10.1007/s10854-018-0523-x

The impact of Eu^{3+} ion substitution on dielectric properties of $Y_{3-x}Eu_xAl_5O_{12}$ ($0.00 \le x \le 0.10$) ceramics

M. A. Almessiere[1,3] · B. Unal[2] · A. Baykal[3] · I. Ercan[4] · M. Yildiz[5]

Received: 29 October 2018 / Accepted: 5 December 2018 / Published online: 10 December 2018

Abstract
This study reported the effect of Eu substitutions on the conductivity and dielectric properties of $Y_{3-x}Eu_xAl_5O_{12}$ ($0.0 \le x \le 0.1$), YAG:xEu^{3+}. All products were fabricated by solid state route. The formation of YAG was approved through X-ray diffraction powder diffraction and high-resolution transmission electron microscope. It was found that the lattice parameters are increasing with increase the substitution content due to the difference in ionic radii between Y^{3+} and Eu^{3+}. Electrical and dielectric properties of YAG ($Y_3Al_5O_{12}$) and YAG:xEu^{3+} ceramics were investigated extensively for a variety of concentrations ($0.00 \le x \le 0.1$) of the substitutional Eu^{3+} ion from the 4f lanthanide group. The temperature dependence of dielectric loss, dielectric constant, loss tangent and *ac*/*dc* conductivity were examined up to 5.0 MHz to understand the electrical and dielectric properties for both doped and undoped YAG ceramics. The experimental results revealed that Eu^{3+} ion substitutions (especially $x = 0.05$) in YAG ceramics meaningfully influence the lossy mechanisms, conductivity and dielectric constant which is probably due to the contribution to the conduction mechanism of the 4*f*–Eu and 3*d*–Al ions. So, this can be incorporated at the exceptional sites of both O_h (octahedral) and T_d (tetrahedral) symmetries in YAG: xEu^{3+} ceramics.

1 Introduction

The quick growth in communication equipment has caused a highly request of Microwave dielectric materials for industrialized communication devices [1, 2]. These microwave electronic devices are extensively used a substrate material that have high-quality factor (Q×f) and low dielectric constant ε_r and [3–5]. YAG ceramics were presupposed to be convenient candidate for this type of application caused by the low ε_r and high-quality factor Q×f at room temperature that revealed that YAG ceramics are in good in terms of microwave dielectric property [6]. These properties due to the ceramics have pores, additional phases with grain boundary, which effected the dielectric loss [7]. Moreover, it is reported that YAG has lower electrical conductivity more than any of polycrystalline oxide [8, 9]. Rare earth oxides doped YAG offered a significant modification in their structure and dielectric performance that are important in many technological applications [10–12]. Doped YAG has been prepared via various approaches such as solvothermal, co-precipitation, hydrothermal, sol–gel, glycothermal and solid-state reaction routes [10, 11, 13–16]. Up to the present time, there is a lack in the studies on the dielectric properties of oxides doped YAG ceramics. In this work we successfully prepared Eu doped YAG by solid-state reaction and investigated the dielectric and microstructural properties in detail.

✉ M. A. Almessiere
malmessiere@iau.edu.sa

1 Department of Physics, College of Science, Institute for Research & Medical Consultations (IRMC), Imam Abdulrahman Bin Faisal University, P.O. Box 1982, Dammam 31441, Saudi Arabia

2 Department of Software and Computer Engineering, Istanbul Sabahattin Zaim University, Halkali Cad. No: 2, 34303 Halkali-Kucukcekmece, Istanbul, Turkey

3 Department of Nanomedicine Research, Institute for Research & Medical Consultations (IRMC), Imam Abdulrahman Bin Faisal University, P.O. Box 1982, Dammam 31441, Saudi Arabia

4 Department of Biophysics, Institute for Research & Medical Consultations (IRMC), Imam Abdulrahman Bin Faisal University, P.O. Box 1982, Dammam 31441, Saudi Arabia

5 Corrosion Research Laboratory, Department of Mechanical Engineering, Faculty of Engineering, Duzce University, 81620 Duzce, Turkey

2 Experimental

2.1 Preparation and characterization

Y_2O_3, Eu_2O_3 and Al_2O_3 are all 99.9% purity and obtained from US-Nano. They were used as initial chemicals the fabrication of $Y_{3-x}Eu_xAl_5O_{12}$ ($0.00 \le x \le 0.1$) ceramics through solid-state route. The metal oxides were mixed and ground by an agate mortar for 30 min. to 1 h until obtaining a homogeneous mixture. Each sample undergoes the same process separately. The mixture was pelletized via a hydraulic press under pressure of about 60 kg/m^2 for 80 s. The pelletizing helps to increase the contact area between grains. After grinding and pelletizing the mixture are prepared for heat treatment process, the pellets are placed into a closed alumina crucible. A lid to prevent the contamination closed crucibles and the pressure caused by the lid can be another factor that guarantee the completion of the reaction. Heating processes will be in three stages and among each heating step; pellet was grinded, made pellet again. First sintering temperature of about 1300 °C for 12 h. Then the samples were grinded and peptized to prepare them to the second stage at 1500 °C for 4 h. The Final stage is about 1600 °C for 2 h. The phase identification of all products was done by X-ray powder diffraction using Rigaku Bench type X-ray powder diffractometer (Cu K_α radiation). FEI Titan S/TEM microscope operating up to 300 kV coupled with an EDXS Si (Li) detector was used for morphological, microstructural analyses. Novocontrol Alpha-N high-resolution dielectric-impedance analyzer was used for the electrical and dielectric measurements of the products.

3 Results and discussion

3.1 Phase investigation

XRD patterns of $Y_{3-x}Eu_xAl_5O_{12}$ ($0.00 \le x \le 0.1$) ceramics are shown in Fig. 1 that shows the well-crystalline YAG phase with the presence of weak $YAlO_3$ (YAP) phase. Moreover, the XRD pattern of doped samples with a low europium concentration ranging from 0.01 to 0.1% display a shift toward smaller angles compared with un-doped sample. The crystalline structure of $Y_{3-x}Eu_xAl_5O_{12}$ ($0.00 \le x \le 0.1$) ceramics were confirmed by Rietveld refinement using Match3! software. The cubic structure was confirm as shown in Table 1. In fact, as the Eu^{3+} ions concentration increases the lattice parameters increases too, almost with a linear relationship. This result is due to the difference between the ionic radius of Eu^{3+} (0.947 Å) ions which is bigger than Y^{3+} ions (0.90 Å). This causes an increase in the lattice parameter as displayed in Table 1.

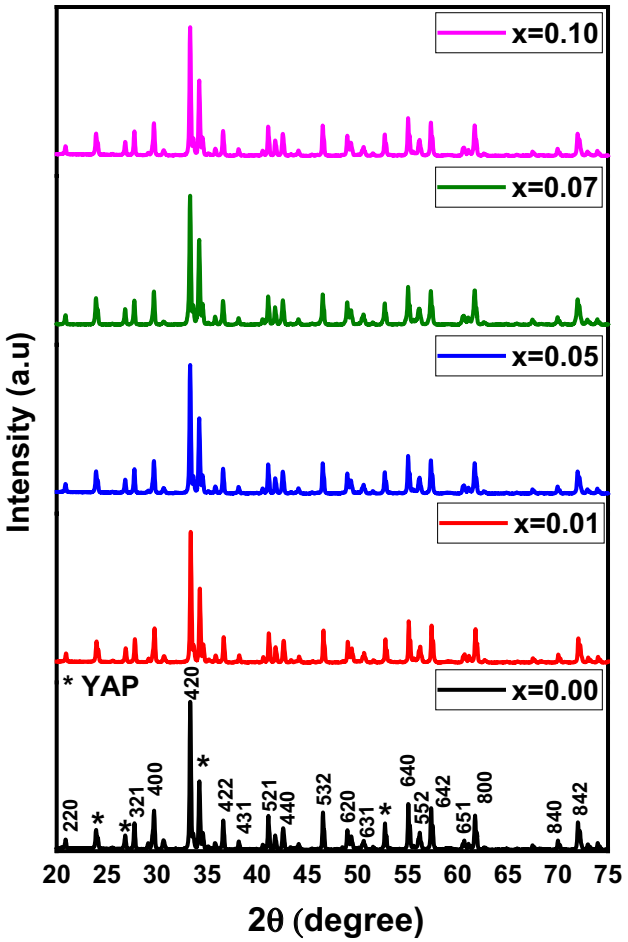

Fig. 1 XRD powder patterns of $Y_{3-x}Eu_xAl_5O_{12}$ ($0.00 \le x \le 0.1$) ceramics

Table 1 Structural and statistical parameters of $Y_{3-x}Eu_xAl_5O_{12}$ ($0.00 \le x \le 0.1$) ceramics obtained by Rietveld refinement

x	a = b = c (Å)	V (Å^3)
0.00	12.0044 (±0.0003)	1730.46
0.01	12.0057 (±0.0002)	1730.59
0.05	12.0072 (±0.0003)	1731.11
0.07	12.0110 (±0.0004)	1732.80
0.10	12.0120 (±0.0005)	1733.18

3.2 Morphology and microstructure analysis

The microstructure of $Y_{3-x}Eu_xAl_5O_{12}$ ($0.00 \le x \le 0.1$) ceramics are presented in Fig. 2. The intermediate magnification SEM images exhibited aggregates of nearly cubic like structure grains. Moreover, the images displayed randomly oriented and well-defined grain boundaries with homogeneous distributed through the sample surfaces. The EDX

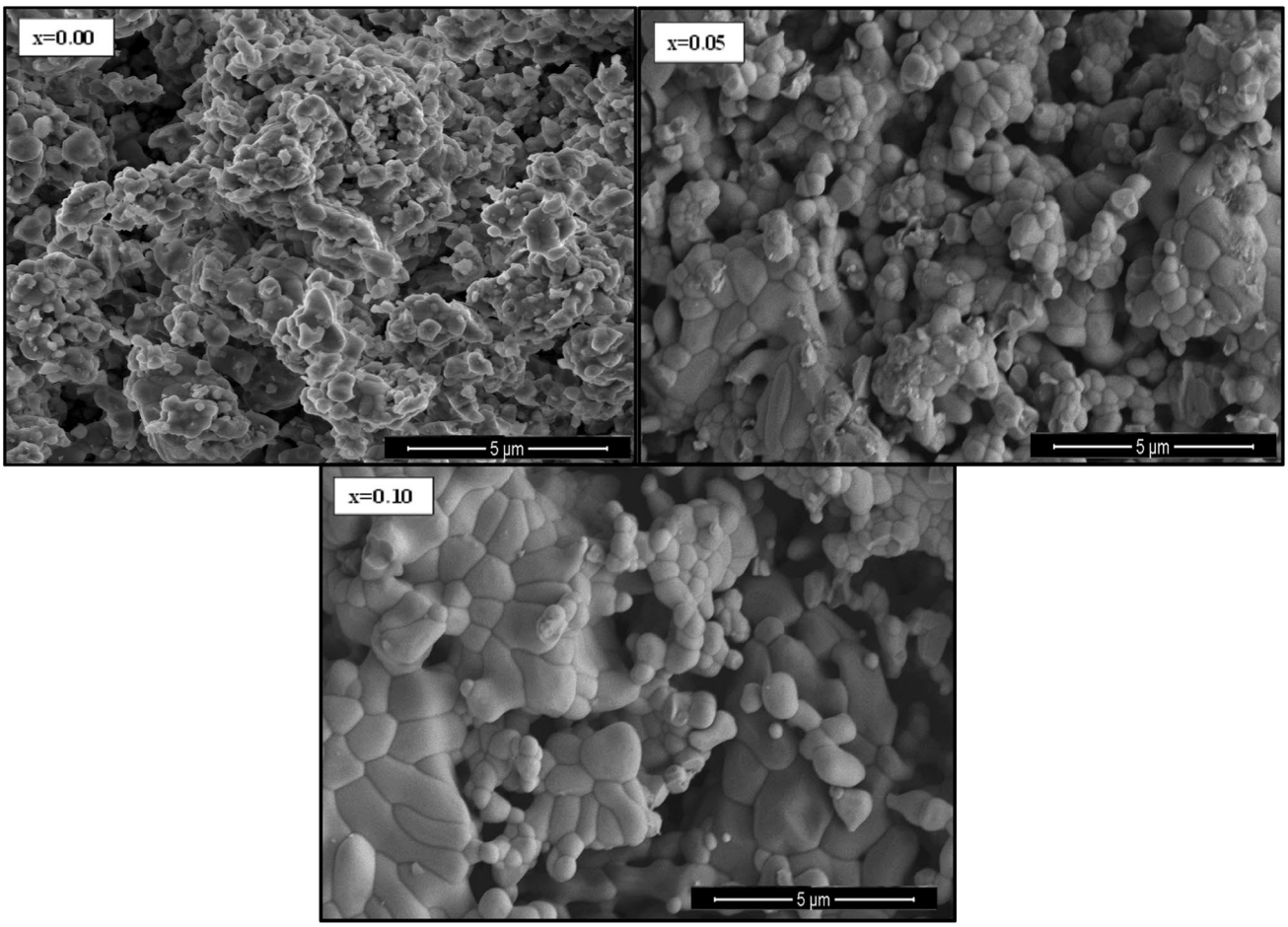

Fig. 2 SEM images of $Y_{3-x}Eu_xAl_5O_{12}$ ($0.00 \le x \le 0.1$) ceramics

and elemental mapping spectra confirmed the formation and chemicals composition of Eu doped YAG ceramics as listed in Fig. 3. The TEM and HR-TEM approved the cubic -like structure of YAG with minor presence of YAP phase according to the d-spacing that observed YAG (220) and (420) and YAP (121) and (222) as seen in Fig. 4.

3.3 Electrical conductivity and dielectric properties

In general, the conductivity could contain two modules in most lanthanide compounds such as $Y_{3-x}Eu_xAl_5O_{12}$. The first module is *dc* conductivity component, which is a result of "band conduction". The second module is *ac* conductivity component, which can be attributed to the "hopping conduction", such as aluminium atom ions of the similar type occurring in multiple valence states. It can be some evidence for this that a certain level of power law dependency is to be represented in the following section. Over the perspectives of theoretical evaluations mentioned earlier, the *ac*/*dc* conductivity, dielectric constant and loss as well as tangent loss all were examined as functions of frequency of the range up to 3.0 MHz, substitutional ratios of x = 0.00, 0.05, 0.07, 0.10, and temperatures up to 120 °C using an impedance analyser [17, 18].

3.4 Conductivity analysis

The electrical conductivity of $Y_{3-x}Eu_xAl_5O_{12}$ ($0.00 \le x \le 0.10$) ceramics was measured as a function of frequency up to 3.0 MHz at a temperature range up to 120 °C as reported earlier. The frequency dependence of Eu-doped YAG ceramics in Fig. 5 on conductivity is calculated from a typical equation expressed as [19],

$$\sigma'(\omega;T) = \sigma_{ac}(\omega;T) = \varepsilon''(\omega;T)\omega\varepsilon_0$$

where, $\sigma'(\omega;T)$ is the real part of complex conductivity, ε'' is the imaginary part of complex dielectric permittivity (ε^*), ε_0 is the vacuum permittivity.

It can be clearly seen from Fig. 5 that both YAG and YAG:xEu^{3+} ($0.01 \le x \le 0.10$) ceramics reveal a linear tendency at two frequencies in log–log plots, regardless of the level of Eu ion substitutional ratios, which indicates that

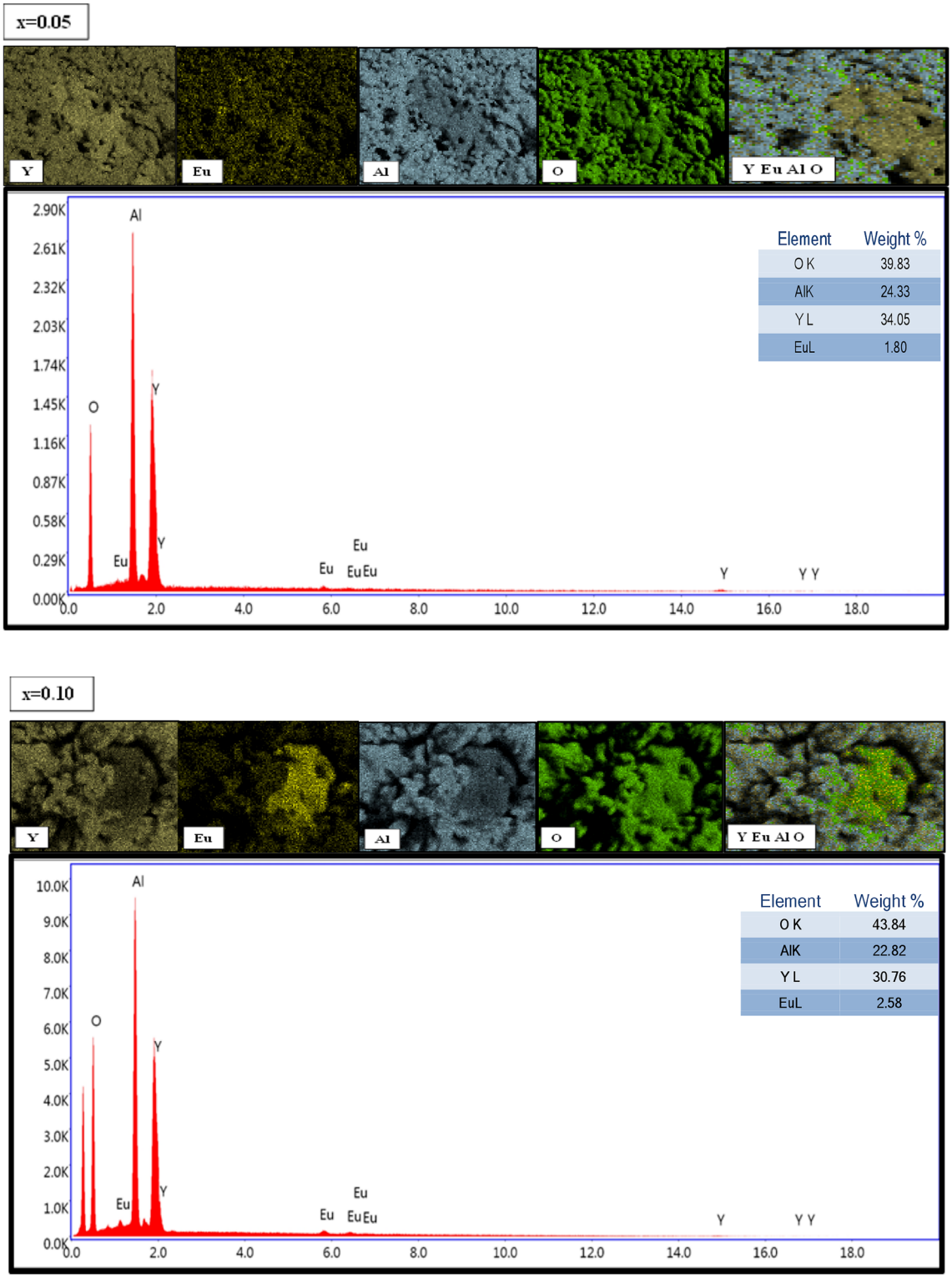

Fig. 3 EDX and elemental mapping spectra of $Y_{3-x}Eu_xAl_5O_{12}$ (x = 0.05 and 0.10) ceramic

conductivity tends to change with a power law exponent under frequency given as follows;

$$\sigma(\omega, T, x) = \sigma_0(T, x)\omega^n$$

where, $\sigma_0(T, x)$ stands for both temperature and dopant-dependent coefficient, and $n(T, x)$ is the power law exponent depending upon both temperature and substitutional level.

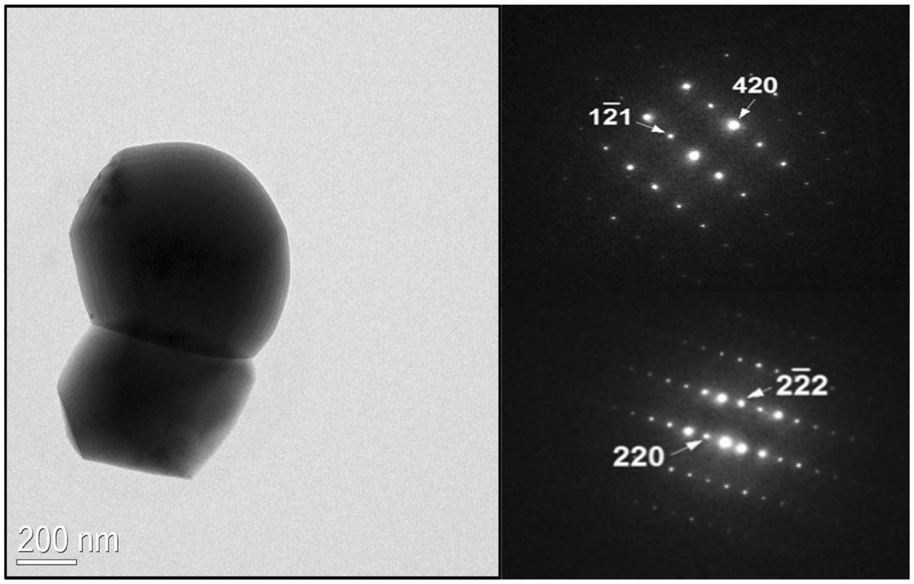

Fig. 4 TEM and HR-TEM images of $Y_{3-x}Eu_xAl_5O_{12}$ (x = 0.05) ceramics

It is also noted that the power exponent varies with doping level and interested frequency ranges of two before and after 1 kHz and 10 kHz. So, power law exponent is evaluated easily from the slope of each curve in a plot of $log\sigma_{ac}$ versus $log\omega$ for each of four ratios for Eu ion substitutions. At low frequency region of < 1 kHz for YAG and YAG:0.05Eu^{3+}; and < 10 kHz for YAG:$x$$Eu^{3+}$ (x = 0.01; 0.07 and 0.10) the power exponent, n is found to be around 0.6 while in high frequency side n is calculated to be a value between 1.56 and 2.00. At some certain frequencies, conductivity origin can be modified easily with level of substitutional Eu^{3+} ions. It can be emphasized that the power law exponent demonstrates some variations at a transition frequency of about 1 kHz for pure and x = 0.05, and 10 kHz for others.

The dispersion in conductivity of both YAG and YAG:0.05Eu^{3+} ceramics in mid-frequency region is quite remarkable because in other Eu^{3+} ion doped ceramics, the characteristic tendencies relative to two-frequency region is more uniform, in which each of the frequency regions seems to obey a power exponent rule. The transition of frequency region occurs at about 1 kHz for both YAG and YAG:0.05Eu^{3+} ceramics, however at about 10 kHz for other YAG:$x$$Eu^{3+}$ (x = 0.01; 0.07 and 0.10) ceramics. The last plot in Fig. 5 shows that *dc* conductivity of YAG:0.10Eu^{3+} is almost independent of temperature while other substitutional level shows a drop-in conductivity similar to the case of YAG ceramics.

The temperature dependence of conductivity of both YAG and YAG:0.05Eu^{3+} ceramics seems to be quite remarkable even though the latter ceramic demonstrates no-transition temperature except for the one owning to a temperature of 120 °C. At certain frequencies below 1.05 kHz it provides numerous insights with an europium ion substitutional effect on conductivity of YAG ceramics. When some type of tendencies for all the curves are discussed carefully, it is clear to note that high dispersion occur for YAG and especially for YAG:0.05Eu^{3+} ceramics. However, the transition frequency shifts to higher side as the dopant concentration increases.

This type of performance could be attributable to some contribution of 'small polaron hopping' to conduction mechanism. This perhaps indicates that the electrical transportation becomes *ac* conduction mechanism owing to the hopping of charge carriers among certain sites. In general, the YAG conductivity declines quickly according to any substitutional rates of Eu^{3+} ions while the conduction depends on both temperature and frequency dependency. This type of tendencies could be taken into account for a common dielectric behaviour [20, 21]. It can be evaluated that the hopping mechanism contributes to some *conduction* enhancements at higher frequencies as some charge carriers are distributed from different trapping centres. So the electron conduction is supported in hopping among octahedral and tetrahedral symmetries of aluminium as mentioned earlier for an overall conduction mechanism. Addition to the above interpretation, there is no much information on the bases of dielectric properties for YAG: $x$$Eu^{3+}$ ceramics in literature apart from some studies in its optical properties [22, 23].

3.5 Dielectric properties: dielectric constant

The evaluation of dielectric parameters such as the dielectric constant and loss, as well as loss factor offers some useful information about the behaviour of electric charge carriers for understanding conduction mechanism in YAG:xEu ceramics. Dielectric measurements of both YAG and YAG:xEu ceramics were performed in a frequency range from 1.0 Hz to 3.0 MHz at a temperature range up to 120 °C.

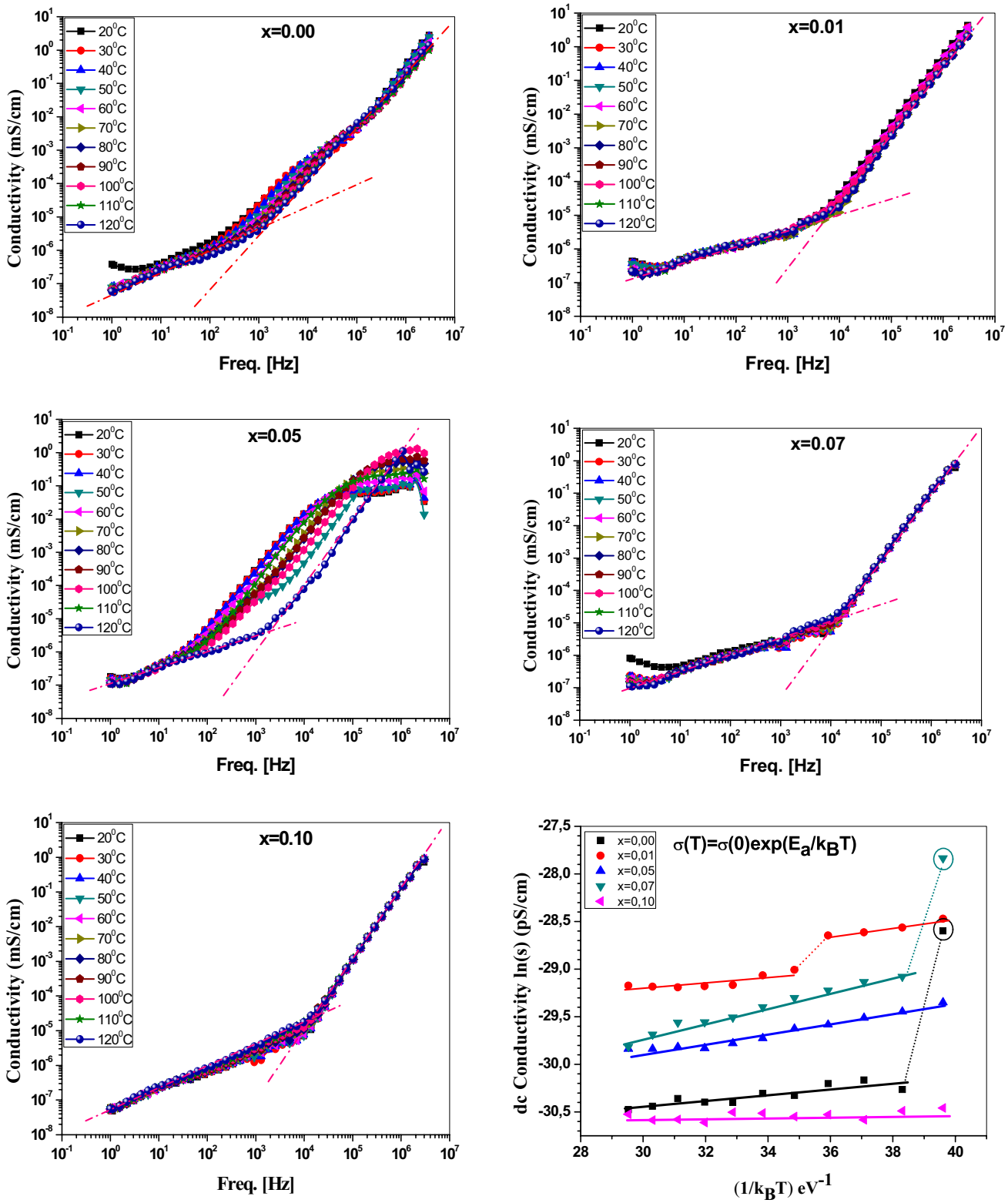

Fig. 5 *ac* conductivity measurements of Eu^{3+} ion doped Yttrium Aluminium Garnet (YAG:*x*Eu ($0.00 \leq x \leq 0.10$)) versus frequency for a range of temperatures up to 120 °C

Generally, the dielectric constant presents very different tendencies over all Eu^{3+} ion substitutions with an incremental frequency up to 3.0 MHz. Temperature dependencies of dielectric constants also show independent variability over the incremental substitutions of Eu^{3+} ions in YAG ceramics. So, the enhancement of dielectric constant is achieved by a regulation of substitutional level of any lanthanide ions in YAG.

The characteristics of dielectric constant of YAG:xEu ($0.00 \le x \le 0.10$) ceramics are depicted in both 2D and 3D of Fig. 6 as function of frequencies for a variety of temperatures up to 120 °C. For YAG ceramics, the dielectric constant decreases with increasing frequency, however, it increases with the elevated temperatures. For Eu^{3+} ion substitution of $x = 0.01$, dielectric constant has more dominant fluctuation at lower and higher frequencies while there is no significant variation at medium frequencies although it increases slightly with temperature. Some tendency similarities in dielectric constant were also observed when compared with the one for $x = 0.07$, except for high frequency side. It is also noticed that the characteristic dielectric constant was observed to increase with the elevated temperature for $x = 0.10$ by indicating maximum peak tendencies in the highest side of frequency just below 3.0 MHz. Especially, for $x = 0.05$ substitution, the graph leads to some regular tendencies in dielectric constant for function of frequency up to 3.0 MHz at temperatures up to 120 °C. Initially, the dielectric constant is kept unchanged for a certain frequency of 1.0 kHz for all temperatures, then above that all the curves shift to a higher frequency side with a type of "fall-off" attitude.

When the frequency dependence of dielectric constant is evaluated in details for a variety of temperature dependency, and for a given substitutional ratio including YAG, all the ceramics are found to have completely different characteristics from each other. So, this is attributed to the conduction mechanism in consequence of the contribution of both electron and polaron hopping mechanisms. Owing to the dielectric complexity of a variety of YAG:xEu^{3+} ceramics for both symmetry types, dielectric constant relies on how fast the polarization takes places in ceramics to link with the oscillation frequency of the applied electric field. Whilst frequency is raised up, the polarization orientation decreases. So, the rearrangement of dipole moments necessitates a longer time interval for the response of oscillation according to the orientation of both ionic and electronic polarization, which yields an insignificant reduction in dielectric constant. So, for all the YAG and YAG:xEu ceramics, both reduction rate and tendencies of all the plots vary with a variety of dependencies such as on temperature and frequency as well as substitutional ratio of the Eu^{3+} ions. In addition to above all discrepancies, the frequency dependency reveals the presence of electrode interface polarization, which usually appears in the lower frequency regions. The temperature dependent increase in dielectric constant could be attributed mostly to the molecular re-organisation and molecular orientation [24, 25]. Thus, the dielectric constant of YAG:xEu^{3+} ($0.0 \le x \le 0.10$) ceramics rises up with elevated temperature due to the substitutional enhancement of boundaries within YAG ceramics. In addition above all, the dielectric constant and loss are reported to decreases with increase in Al^{3+} ions [26].The electrical conduction in these YAG ceramics is easily interpreted based on the hopping mechanism. So, the dielectric constant adheres to the Maxwell–Wagner interfacial polarization.

3.6 Dielectric loss

As can be seen from both 2D and 3D plots of Fig. 7, the dielectric loss of both YAG and YAG:xEu^{3+} ceramics displays an exponent power law tendency within a certain frequency region i.e. nearly a linear tendency in *log–log* 2D plots. For $x = 0.01$, 0.07 and 0.10, this linearity over a certain frequency range in *log–log* 2D plots obeys the power law, where the exponent, n is having a positive and negative value, as defined by $\varepsilon''(\omega;T) = \varepsilon''(0;T)\omega^{n}$ for high frequency region above 10.0 kHz and, by $\varepsilon''(\omega;T) = \varepsilon''(0;T)\omega^{-n}$ for low frequency region below 10.0 kHz, where $\varepsilon''(0;T)$ is the pre-coefficient parameter of dielectric loss that is strongly dependent on the temperature. 'n' is the power exponent correlated with temperature and substitutional ratio in YAG:xEu, and also YAG, as illustrated in 2D plots of Fig. 7. Yet, the loss ultimately reaches a minimum at a frequency of about 10.0 kHz. Besides, the characteristic linearity for both YAG and YAG:0.05Eu^{3+} become more complicated. The dielectric loss of YAG ceramics experiences three regional variation with a negative–positive–positive exponent order while the loss curves for YAG:0.05Eu^{3+} ceramics undertake variable behaviour with a negative–positive–negative exponent order, which seems to have high temperature dependency, especially for medium and high frequency regions.

Therefore, the temperature dependent mechanism of dielectric loss can be considered to depend upon the nature of reorganization because of the structural diffusion of ionic substitutions in YAG. It is also evident that the capacitive response exhibits a higher temperature dependence compared to the nature of reorganization of Eu^{3+} ions in YAG. This linearity in *log–log* plots corresponds to *dc* conductance (σ_{dc}), expressed as $\varepsilon''_{dc} = \sigma_{dc}(\omega C_o)$ where, C_o is the vacuum capacitance. Due to charge transfer among both O_h and T_d symmetries of the Al^{3+} ions in YAG ceramics, a restricted drift motion for carrier charges takes place along the orientation of an externally applied electric field, resulting in a type of polarization establishment. The polarization level reduces with an incremental frequency because the electronic type conduction between the octahedral and

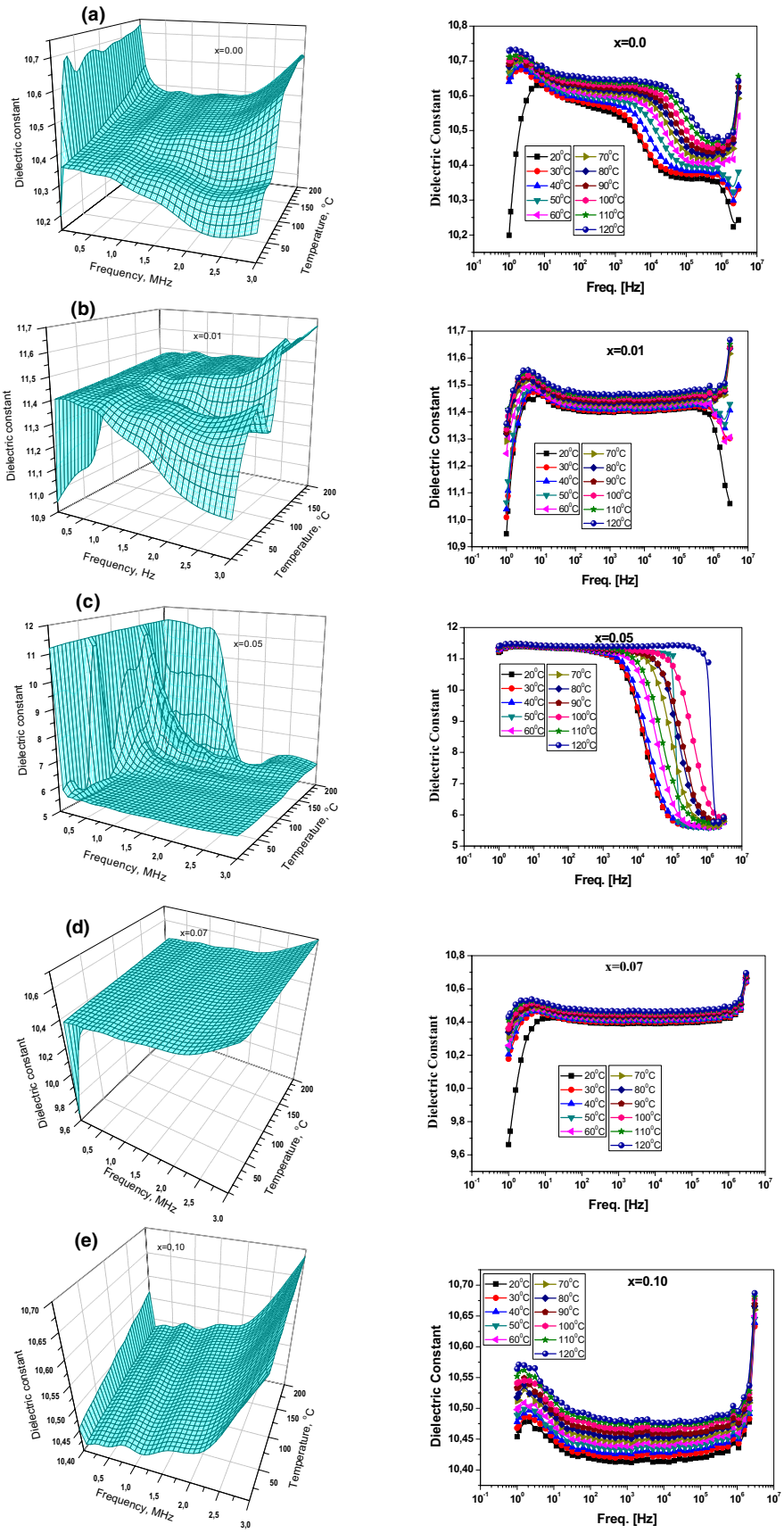

Fig. 6 Two (2D) and three dimensional (3D) plots of temperature and frequency dependence for dielectric constant of Eu^{3+} ion doped Yttrium Aluminium Garnet ceramics (YAG:*x*Eu ($0.00 \leq x \leq 0.10$))

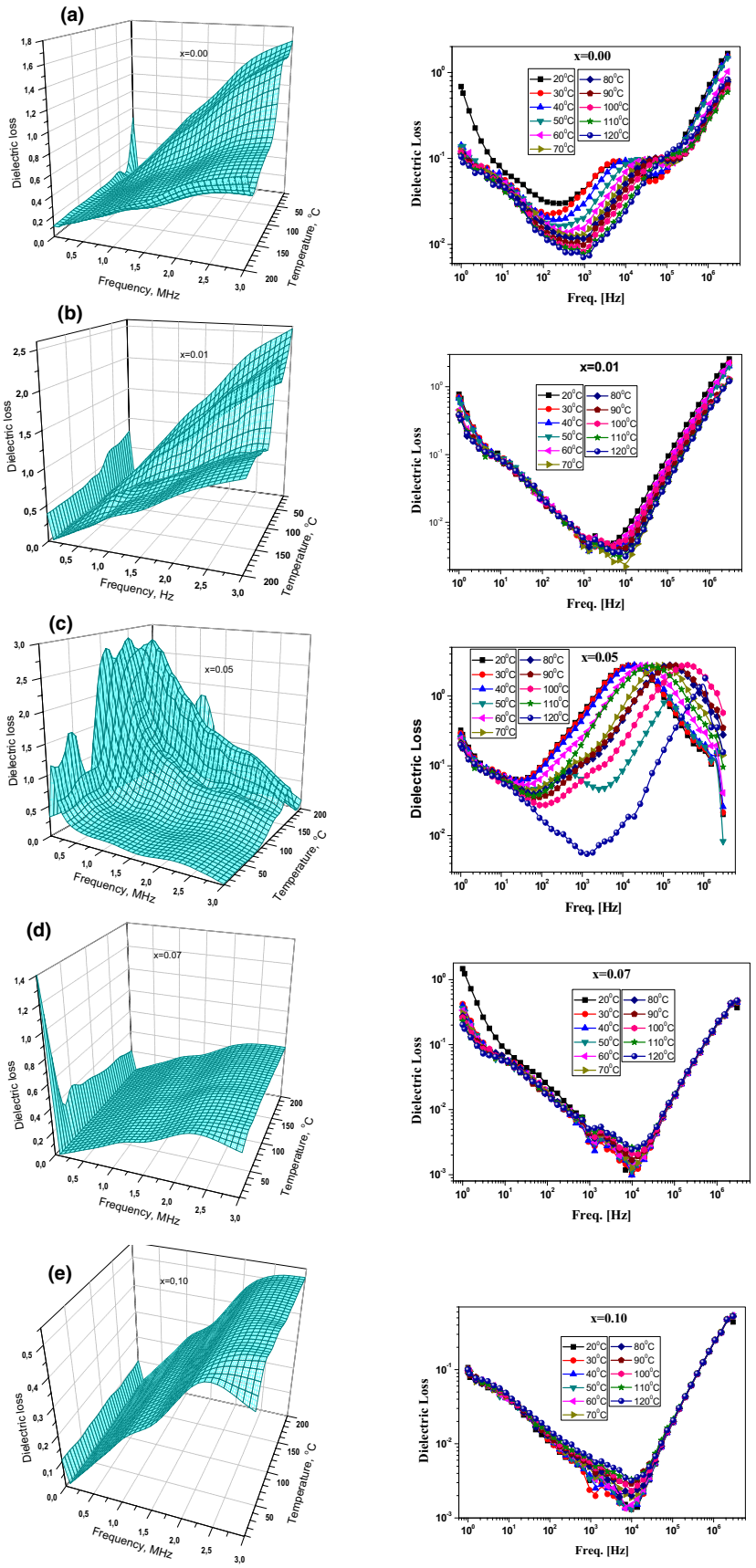

Fig. 7 2D and 3D plots of temperature and frequency dependence of dielectric loss for Eu^{3+} ion doped Yttrium Aluminium Garnet ceramics (YAG:*x*Eu ($0.00 \leq x \leq 0.10$))

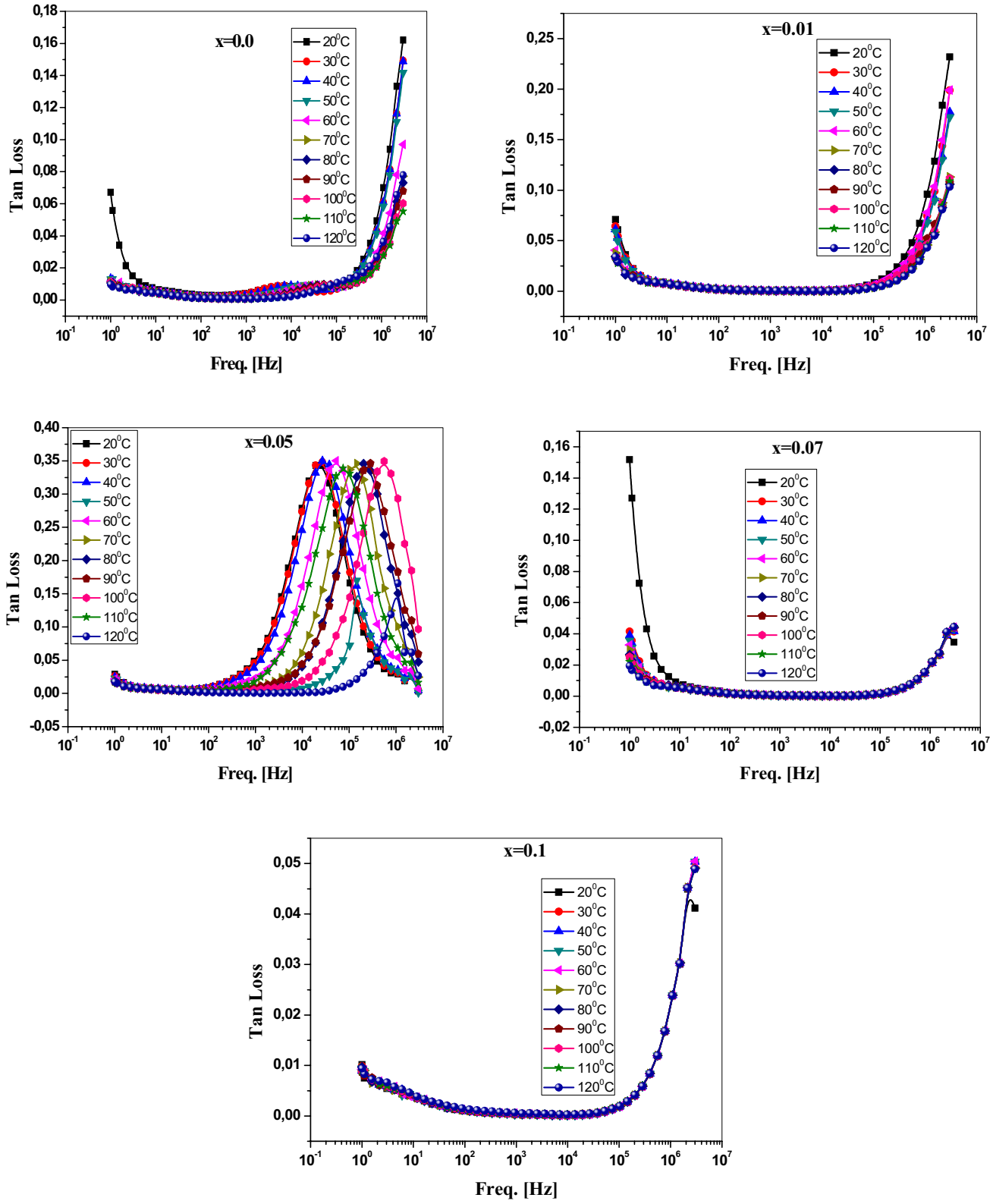

Fig. 8 Dielectric loss tangent characteristics of Eu^{3+} ion doped Yttrium Aluminium Garnet (YAG:*x*Eu ($0.00 \leq x \leq 0.10$)) versus frequency for a range of temperatures up to 120 °C

tetrahedral symmetries suspends the subsequent electric field [26].

In addition above all, the dielectric constant and loss are reported to decreases with increase in Al^{3+} ions [27]. The electrical conduction in these YAG ceramics is easily interpreted based on the hopping mechanism. So, the dielectric constant adheres to the Maxwell–Wagner interfacial polarization.

3.7 Tangent loss

The characteristic representation of dielectric tangent loss of $Y_{3-x}Eu_xAl_5O_{12}$ ($0.00 \le x \le 0.10$) is demonstrated in Fig. 8 as function of frequencies for a range of temperatures up to 120 °C. The dielectric loss tangent evidently declines at first with a multi-exponential approach instead of a single exponential tendency. It is then kept constant up to a certain frequency value for each which is dependent on substitutional ratio except for $x = 0.05$. Finally it increases exponentially with an elevated frequency at the highest side of the plot. However, YAG:0.05Eu ceramic shows a quite different behavior in dielectric loss tangent similar to other characteristic parameters. It is clearly seen for YAG:0.05Eu ceramics in Fig. 8 that dielectric loss tangent possesses a peak value of about 10.0 kHz at a temperature of 20 °C, and then shifts to a high frequency side by increasing temperature up to 120 °C. It should be also noted that peak value is kept constant but shifts to the opposite side at a temperature of 100 °C, then shifts to higher frequency side by dropping to the peak value down to 0.15. It is well known that the frequency dependent reduction in both dielectric constant and tangent loss is a normal behaviour in the octahedral/tetrahedral symmetries of aluminium ions in YAG ceramics, which can be attributed to charge polarization. The reduction in these parameters occurs due to the hopping efficiency of electron replacement between the octahedral and tetrahedral symmetry sites of aluminium atoms in YAG. Thus, this becomes far irrelevant to the stimulation of external electric field. This type of tendencies in dielectric loss tangent provide us with a useful modification, some kind of tuneability adjustability and a variety of modulations for some certain instrumentations such as band-pass filters and some type of laser application in optoelectronics [20, 24, 25].

4 Conclusion

Eu^{3+} Ion substitution YAG has been synthesis via solid state reaction. The resulted compositions are characterized by XRD powder pattern, scanning electron microscope, and high-resolution electron microscope to approve the YAG structure. Dielectric-impedance analyser was implemented for studying dielectric properties. The electrical and dielectric properties of both YAG and Eu:YAG ceramics as functions of frequency for temperature ranges up to 120 °C were evaluated extensively from the perspective of the conduction mechanism. The temperature dependence of dielectric constant, loss tangent, conductivity, dielectric loss up to 3.0 MHz for both types of the ceramics is ascribed to various lattice locations such as 4*f*–Eu and 3*d*–Al ions in both T_d and O_h symmetry in YAG:xEu^{3+} ceramics as well as YAG itself. It is obvious that the reduction of the dielectric constant and the loss tangent by frequency leads to an expected tendency in the O_h/T_d symmetries of Al^{3+} ions in YAG ceramics attributable to the charge polarization.

Acknowledgements Authors are grateful to the Institute for Research & Medical Consultations (IRMC) of Imam Abdulrahman Bin Faysal University for the financial assistance to pursue this research (Grant No: 2018-IRMC-S-1). The technical assistance provided by Core Labs of King Abdullah University of Science and Technology (KAUST) are highly appreciated.

References

1. D. Zhou, C.A. Randall, L.X. Pang, H. Wang, X.G. Wu, J. Guo, G.Q. Zhang, L. Shui, X. Yao, Microwave dielectric properties of $Li_2(M^{2+})_2Mo_3O_{12}$ and $Li_3(M^{3+})_2Mo_3O_{12}$ (M = Zn, Ca, Al, and In) lyonsite-related-type ceramics with ultra-low sintering temperatures. J. Am. Ceram. Soc. **94**, 802–805 (2011)
2. Q.L. Zhang, H. Yang, H.P. Sun, A new microwave ceramic with low- permittivity for LTCC applications. J. Eur. Ceram. Soc. **28**, 605–609 (2008)
3. I.M. Reaney, D. Iddles, I.M. Reaney, D. Iddles, Microwave dielectric ceramics for resonators and filters in mobile phone networks. J. Am. Ceram. Soc. **89**, 2063–2072 (2006)
4. B. Ullah, W. Lei, Z.-Y. Zou, X.-H. Wang, W.Z. Lu, Synthesis strategy, phase-chemical structure and microwave dielectric properties of paraelectric $Sr_{(1-3x/2)}Ce_xTiO_3$ ceramics. J. Alloys Compd. **695**, 648–655 (2017)
5. Z.Y. Shen, Q.G. Hu, Y.M. Li, Z.M. Wang, W.Q. Luo, Y. Hong, Z.X. Xie, R.H. Liao, X. Tan, Structure and dielectric properties of $Re_{0.02}Sr_{0.97}TiO_3$ (*Re* = La, Sm, Gd, Er) ceramics for high-voltage capacitor applications. J. Am. Ceram. Soc. **96**, 551–2555 (2013)
6. J. Krupka, K. Derzakowski, M. Tobar, J. Hartnett, R.G. Geyer, Complex permittivity of some ultra-low loss dielectric crystals at cryogenic temperatures. Meas. Sci. Technol. **10**, 387–392 (1999)
7. Q. Liu, J. Liu, J. Li, et al., Solid-state reactive sintering of YAG transparent ceramics for optical applications. J. Alloys Compd. **616**, 81–88 (2014)
8. J.M. Yang, S.M. Jeng, S. Chang, Fracture behavior of directionally solidified $Y_3Al_5O_{12}/Al_2O_3$ eutectic fiber. J. Am. Ceram. Soc. **79**, 1218 (1996)
9. A. Kareiva, J. Harlan, C.B. MacQueen D, R.L. Cook, A.R. Barron, Carboxylate-substituted alumoxanes as processable precursors to transition metal—aluminum and lanthanide—aluminum mixed-metal oxides: atomic scale mixing via a new transmetalation reaction. Chem. Mater. **8**, 2331 (1996)
10. R. Asakura, T. Isobe, K. Kurokawa, T. Takagi, H. Aizawa, M. Ohkubo, Effects of citric acid additive on photoluminescence properties of YAG: Ce^{3+} nanoparticles synthesized by glycothermal reaction. J. Lumin. **127**, 416–422 (2007)

11. X. Li, H. Liu, J. Wang, H. Cui, F. Han, YAG:Ce nano-sized phosphor particles prepared by a solvothermal method. Mater. Res. Bull. **39**, 1923–1930 (2004)
12. Y. Hakuta, T. Haganuma, K. Sue, T. Adschiri, K. Arai, Continuous production of phosphor YAG:Tb nanoparticles by hydrothermal synthesis in supercritical water. Mater. Res. Bull. **38**, 1257–1265 (2003)
13. G. Seeta, R. Raju, H.C. Jung, J.Y. Park, J.W. Chung, B.K. Moon, J.H. Jeong, S.M. Son, J.H. Kim, Sintering temperature effect and luminescent properties of Dy^{3+}: YAG nanophosphor. J. Optoelectron. Adv. Mater. **12**(6), 1273–1278 (2010)
14. H.M.H. Fadlalla, C.C. Tang, E.M. Elssfah, F. Shi, Synthesis and characterization of single crystalline YAG: Eu nano-sized powder by sol–gel method. Mater. Chem. Phys. **109**, 436–439 (2008)
15. M.L. Saladino, E. Caponetti, Co-precipitation synthesis of Nd: YAG nanopowders II: the effect of Nd dopant addition on luminescence properties. Opt. Mater. **32**, 89–93 (2009)
16. W. Jin, W. Yin, S. Yun, M. Tang, T. Xu, B. Kang, H. Huang, Microwave dielectric properties of pure YAG transparent ceramics. Mater. Lett. **173**, 47–49 (2016)
17. S. Maletic, D. Popovic, D. Cerovic, J. Dojcilovic, Study of structural and spectral characteristics of crystal $Y_3Al_5O_{12}$, Al_2O_3 and $SrTiO_3$ doped by 3d- or 4f- ions. Contemp. Mater. **2**, 190 (2016)
18. I.A. Auwal, B. Unal, H. Güngüneş, S.E. Shirsath, A. Baykal, Dielectric properties, cationic distribution calculation and hyperfine interactions of La^{3+} and Bi^{3+} doped strontium hexaferrites. Ceram. Int. **42**, 9100 (2016)
19. E. Talebian, M. Talebia, A general review on the derivation of Clausius–Mossotti relation. Optik **124**, 2324 (2013)
20. M.A. Almessiere, B. Unal, A. Baykal, Dielectric and microstructural properties of YAG:Dy^{3+} ceramics. J. Rare Earths (2018) https://doi.org/10.1016/j.jre.2018.04.011 (**In press**)
21. M.A. Almessiere, N.M. Ahmed, I. Massoudia, A.L. Al-Otaibia, A.A. Al-shehria, M. Al Shafouri, Study of the structural and luminescent properties of Ce^{3+} and Eu^{3+} co-doped YAG synthesized by solid state reaction. Optik **158**, 152–163 (2018)
22. X. Niu, J. Xun, Y. Zhang, The spectroscopic properties of Dy^{3+} and Eu^{3+} co-doped $Y_3Al_5O_{12}$ (YAG) phosphors for White LED. Progr. Nat. Sci. **25**, 209–214 (2015)
23. M. Skruodiene, M. Misevicius, M. Sakalauskaite, A. Katelnikovas, R. Skaudzius, Doping effect of Tb^{3+} ions on luminescence properties of $Y_3Al_5O_{12}$: Cr^{3+} phosphor. J. Lumin. **179**, 355–360 (2016)
24. Y. Zhou, J. Lin, M. Yu, S. Wang, Comparative study on the luminescent properties of $Y_3Al_5O_{12}$:RE^{3+} (RE: Eu, Dy) phosphors synthesized by three methods. J. Alloys Compd. **375**, 93 (2004)
25. S.A. Hassanzadeh-Tabrizi, Low temperature synthesis and luminescence properties of YAG:Eu nanopowders prepared by modified sol-gel method. Trans. Nonferrous Met. Soc. China **21**, 2443 (2011)
26. Q. Liu, Y. Yuan, J. Li, J. Liu, C. Hu, M. Chen, L. Lina, H. Kou, Y. Shi, W. Liu, H. Chen, Y. Pan, J. Guo, Preparation and properties of transparent Eu:YAG fluorescent ceramics with different doping concentrations. Ceram. Int. **40**, 8539–8545 (2014)
27. S. Verma, J. Chand, M. Singh, Mössbauer, magnetic, dielectric and dc conductivity of Al^{3+} ions substituted Mg-Mn-Ni nano ferrite synthesized by citrate precursor method". Adv. Mater. Lett. **4**, 310 (2013)